Desalination and Water Treatment
www.deswater.com

doi: 10.1080/19443994.2015.1060539

57 (2016) 13415–13424
June

Taylor & Francis
Taylor & Francis Group

Fouling of forward osmosis membrane by protein (BSA): effects of pH, calcium, ionic strength, initial permeate flux, membrane orientation and foulant composition

Pin Zhao[a], Baoyu Gao[a], Qinyan Yue[a,*], Ho Kyong Shon[b], Qian Li[a]

[a]*Shandong Provincial Key Laboratory of Water Pollution Control and Resource Reuse, School of Environmental Science and Engineering, Shandong University, Jinan 250100, China, Tel. +86 15806625680; email: wszplak@163.com (P. Zhao), Tel. +86 531 88365258; Fax: +86 531 88364513; emails: baoyugao_sdu@aliyun (B. Gao), qyyue58@aliyun.com (Q. Yue), qianli@sdu.edu.cn (Q. Li)*

[b]*School of Civil and Environmental Engineering, University of Technology, P.O. Box 129. Broadway 2007, Sydney (UTS), NSW, Australia, email: Hokyong.Shon-1@uts.edu.au*

Received 10 February 2015; Accepted 31 May 2015

ABSTRACT

In this study, bovine serum albumin (BSA) was selected to represent proteins of secondary wastewater effluent. The role of various physical and chemical interactions, such as calcium concentration, ionic strength, solution pH, feed foulant composition, initial permeate flux, and membrane orientation, in BSA fouling of forward osmosis (FO) membranes was investigated. Fouling experiments showed that membrane fouling by BSA was enhanced with increasing calcium concentration and ionic strength. The former was mainly due to the complexes formed by the interaction of Ca^{2+} and carboxylic functional groups of BSA, and the latter resulted from the decreasing electrostatic repulsion among BSA molecules and between BSA molecules and membrane. Moreover, FO membrane fouling became much more significant at solution pH 4.7 (the BSA isoelectric point), where BSA molecules were neutrally charged and had no electrostatic repulsion among themselves. It was also demonstrated that the presence of alginate (a model polysaccharide) as co-foulant aggravated the BSA fouling of FO membrane, which could be attributed to the remarkable contribution of the alginateBSACa^{2+} complexes within the fouling layer to the total membrane resistance. The fouled membranes were examined by scanning electron microscopy to further sustain the conclusion. In addition, the size distribution of foulant molecules in various FS was measured and used as a reference to judge and control the behavior of BSA fouling. The present paper is contributed to better understanding of FO membrane fouling caused by protein (BSA) and has instructive significance for the future development.

Keywords: Forward osmosis; Membrane fouling; Protein fouling; Bovine serum albumin; BSA; Size distribution

*Corresponding author.

1. Introduction

Over the last few decades, fresh water scarcity issues have become more and more severe due to industrialization, population growth and climate change [1]. Forward osmosis (FO), a novel and emerging low-energy friendly membrane technology, has been gaining popularity in recent years [2]. Instead of requiring hydraulic pressure, FO happens automatically due to concentration or osmotic gradient between the two sides of semi-permeable membrane and achieves high rejection of a wide range of contaminants [3,4].

Since the lack of applied hydraulic pressure, the fouling in the FO process is proven to be lower and irreversible. In addition, the FO fouling mechanisms are quite different from that in the pressure-driven membrane processes [5–8]. The fouling mechanisms of microfiltration membranes by proteins have been elucidated clearly, which is proven to be attributed to membrane pore blocking and/or pore constriction during initial fouling, followed by cake formation on the membrane surface during long-term fouling [9–11]. Additionally, the fouling mechanisms of RO membrane was investigated by W. Ang and M. Elimelech and determined that the feed solution (FS) chemistry (calcium concentration, ionic strength, and solution pH) and feed foulant composition would influence membrane fouling [12]. Lee et al. [13] compared the fouling behavior of FO and RO, and demonstrated that the structure (i.e. thickness and compactness) of the fouling layers of FO and RO was quite different. Moreover, in FO, the fouling was effected dramatically by the type of organic foulant, size of colloidal foulant, and the type of the draw solution (DS). Mi and Elimelech studied that the coupled influence of chemical and hydrodynamic interactions on the membrane fouling in FO process by choosing three model organic foulants, and then found that bovine serum albumin (BSA) had weak intermolecular interactions and formed cake layer only at the most favorable hydrodynamic conditions [14,15].

Proteins, as common large molecules, widely exist in secondary wastewater effluent. As presented in the previous papers, protein fouling is one of the critical factors governing the effectiveness of membrane processes. However, the underlying chemical and physical mechanisms that influence its fouling behavior have not been clearly and fully established in the FO process. In particular, the pH affects the charge characteristics of protein dramatically, but the effects of pH on protein fouling have been studied less during the FO process. In this paper, BSA was selected as model organic foulants to represent protein. The BSA fouling mechanisms were fully studied in the FO process. Specifically, the influence of FS chemical characteristics, such as calcium concentration, ionic strength, solution pH and feed contaminant composition (proportions of BSA to sodium alginate (common polysaccharides) by mass concentrations) and physical factors, for instance, initial permeate flux and membrane orientation were studied. Moreover, the size of foulant molecules was measured and used as a reference to judge and control the fouling behavior. Particularly necessary to note is the molecule conformations of the BSA controlled by the solution pH which will affect the fouling behavior.

2. Materials and methods

2.1. Organic foulant

BSA and sodium alginate were chosen to be model organic foulants to represent protein and common polysaccharides, respectively. BSA was provided by Klontech Company from Roche. The weight of the BSA is approximately 68 kDa. Its purity is more than 96%. Water content is less than 5%. BSA is reported to have an isoelectric point at pH 4.7 [16]. Sodium alginate was obtained from Sinopharm Chemical Reagent Co., Ltd. (Shanghai). It is analytically pure. The molecular weight is 12–80 kDa.

Stock solutions of BSA and sodium alginate (2 g/L) were as prepared by dissolving the organic foulant (received in powder form) in deionized (DI) water and mixing for over 12 h to ensure complete dissolution. The stock solution was stored in sterilized glass bottles at 4℃ without further purification.

2.2. Test solutions

For fouling experiments, the FS contained NaCl and 200 mg/L foulant, some also contained $CaCl_2$. The pH was adjusted by the 1 M NaOH or 1 M HCl. The DS was composed of 1.5 or 4 M NaCl. The osmotic pressures of the 10 mM NaCl feed and 1.5/4 M NaCl draw solutions were predicted using OLI Systems analyzer and determined to be 0.3543 and 72.56/231.14 atm, respectively. The partical size of FS in different situations was measured by Zetasizer Nano Analyzer.

2.3. FO membrane

The membrane used in this study is a commercial flatsheet cellulose triacetate (CTA) FO membrane (Hydration Technology Innovations or HTI, Albany,

USA), which has been widely used for FO process in wastewater reclamation applications. The CTA membrane shares the general characteristics of asymmetric structure which is made from cellulose acetate embedded in a polyester woven mesh. More information on the properties and characteristics are presented in Table 1. The membrane is relatively hydrophilic and negatively charged at pH 6 of FS [17,18]. The pure water permeability coefficient was measured under hydraulic pressure (RO mode) and determined to be 0.98 L/(m^2 h bar).

2.4. Membrane orientation

Since the absence of hydraulic pressure in FO processes, there are two modes of membrane orientation in FO process. Specifically, the first one is the membrane porous layer facing the FS and the dense layer facing the DS, which is referred to as the pressure-retarded osmosis (PRO) mode, whereas the DS is placed against the support layer and the dilute FS is on the active layer, which is the other one referred to as the FO mode.

2.5. FO system and fouling experiments

The fouling tests were conducted using bench scale flatsheet cross-flow FO system, which was similar to the unit used in our earlier studies [19]. It contained a flat membrane sheet placed in a rectangular channel with internal dimensions 7.7 cm long, 2.6 cm wide and 0.3 cm high. 1.5 and 4 M NaCl were employed as DS to obtain different initial fluxes. A weighing balance (Satorius weighing technology GmbH, Gottingen, Germany) was used to record the variation in the DS weight for water flux computation.

For the experimental protocol, the membrane was immersed in DI water for 12 h. Then, 1 L FS with foulant and 1 L DS were added to the feed and draw tank, respectively. After reaching the desired temperature, 25˚C, the bypass valves of both cross-flows were closed to allow flow of FS and DS through both sides of the membrane. The cross-flow velocities for both the feed and draw sides were fixed at 8.5 cm/s. After the data stabilized, which took about 10 min, the weighing balance came to counting. The fouling experiment lasted until the permeate volume reached 500 mL.

Baseline experiments were carried out to determine the decline in permeate water flux due to the decrease in the osmotic driving force during the fouling experiments, which was attributed to the dilution of the DS by the permeate water. The baseline experiments followed the same protocol as that for the fouling experiments except that no foulant was added to FS.

3. Results and discussion

3.1. Baseline experiments

During the fouling experiments in batch mode, the osmotic gradient between the two sides of membrane keeps decreasing due to the dilution of DS and concentration of FS. Therefore, there are two main factors resulting in the flux decline in the fouling experiments: one is membrane fouling and another is the decrease in osmotic driving force. In order to investigate the effects of fouling on the water flux, the effect of decrease of osmotic driving force must be separated. Baseline experiments was conducted, in which the flux decline that resulted from the progressive decrease in the osmotic driving force was quantified.

The baseline experiments were conducted under conditions corresponding to the fouling experiments, excluding the foulant in the FS (10 Mm NaCl). Fig. 1(a) represents the permeate flux decline as a function of accumulated permeate volume. Furthermore, through a computation based on the dilution of DS by permeate flow, the water flux behavior as a function of the corresponding DS osmotic pressure was obtained and presented in Fig. 1(b).

Table 1
Physical and chemical properties of cellulose triacetate (CTA) membranes as provided by the manufacturer and from various literature sources

Sample	Active layer material	Contact angle (˚)		Zeta potential at pH 6 (mV) active layer	Pure water permeability A (L/(m^2 h bar))	Operating pH	Membrane Thickness (μm)
		Active layer	Support layer				
CTA	Cellulose triacetate	76.6	81.8	−2.1	0.98	3–8	93

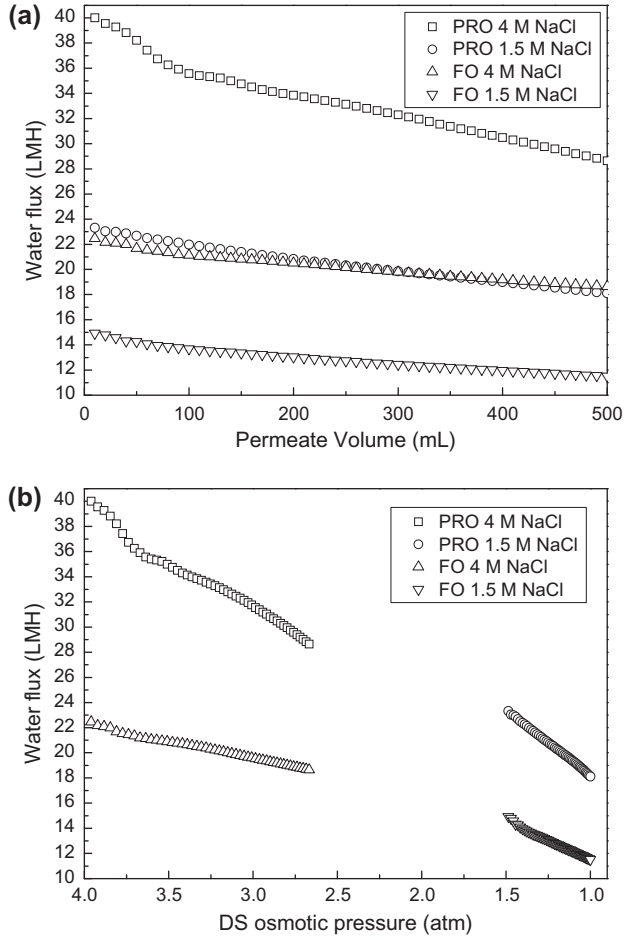

Fig. 1. Variation of water flux with (a) the accumulated permeate volume and (b) the corresponding osmotic pressure of the DS in the baseline test. The FS and DS initially contain 10 mM NaCl and 4.0/1.5 M NaCl, respectively. Other test conditions: cross-flow velocity of 8.5 cm/s, pH of 6.4 ± 0.1, and temperature of 25 ± 1 ℃.

As shown in Fig. 1(a), the water flux in the PRO mode was higher than that in the FO mode under the same condition. Specially, the flux of 1.5 M NaCl in the PRO mode was approximately equal to that of 4 M NaCl in the FO mode. It can be clearly seen from Fig. 1(b) that the flux in the PRO mode declined faster than that in the FO mode under the same DS osmotic pressure. This behavior was attributed to internal concentration polarization effects as described in detail in many other publications [18,20]. The flux decline curves listed in Fig. 1 were used as baselines to normalize the flux decline curves obtained from the fouling experiments. Firstly, the baseline flux was first divided by its corresponding initial flux to obtain a normalization factor. Then the normalization factor was subtracted from the flux data from the fouling experiment to obtain the corrected flux, which was only influenced by the membrane fouling. To avoid confusion, there was the corrected flux instead of the actual observed flux in the flux decline curves of the fouling experiments. In other words, the flux decline curves shown in Figs. 2–7 solely represent the effect of membrane fouling.

3.2. Influence of solution chemistry on fouling

3.2.1. Calcium concentration

The presence of carboxylic functional groups in BSA had been reported by other papers [11,21]. As a major divalent cation in natural and waste waters, calcium enhanced BSA fouling in FO systems by interacting and forming complexes with carboxylic functional groups of organic molecules. To study the effect of calcium concentration on BSA fouling of FO membrane, fouling experiments were performed with FSs containing various concentrations of $CaCl_2$, in which the total ionic strength was maintained at 10 mM by adjusting the background NaCl concentration. The flux decline curves obtained for each fouling condition are presented in Fig. 2.

It had been proven that calcium ions enhanced BSA fouling in RO membrane systems [12]. Similar to the RO system, compared to that in the absence of calcium ions, there was an apparent flux decline during BSA fouling in the presence of calcium ions in the FO system. As the Ca^{2+} concentration increased, the water flux decreased correspondingly from 11.4 L/(m^2 h) (LMH) in the absence of Ca^{2+} to 10.78 LMH in the

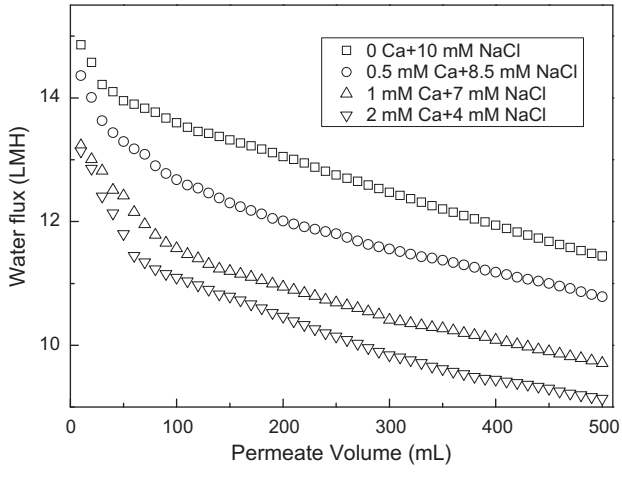

Fig. 2. Effect of calcium concentration on BSA fouling of the FO membrane in the FO mode. Total ionic strength of the FS was fixed at 10 mM by varying NaCl concentration. DS initially contain 1.5 M NaCl.

presence of 0.5 mM Ca^{2+} and then to 9.1 LMH in the presence of 2 mM Ca^{2+}. The results indicated that, the increase of the Ca^{2+} concentration facilitated the combination of Ca^{2+} with carboxylic functional groups of BSA, leading to more severe membrane fouling. On the other hand, at the ambient pH 6.5 ± 0.1, both the BSA molecules and membrane surface were negatively charged, whereas the electrostatic repulsion existed among the BSA molecules and between the molecules and the membrane surface. The presence of Ca^{2+} ions could reduce the electrostatic repulsion through neutralizing charge. In addition, the effect became more significant with increasing Ca^{2+} concentration at a fixed total ionic strength.

In the other hand, there were two stages in the flux–volume curves. The water flux declined rapidly before the 100 mL, and then it declined relatively smoothly. Moreover, the flux declined more smoothly in the second stage in presence of Ca^{2+}. In the first stage, the convective deposition of BSA aggregated on the membrane surface and increased the hydraulic resistance. In the second stage, there were two different situations. The chemical attachment of native BSA caused the protein deposit by forming an intermolecular disulfide linkage in absence of Ca^{2+}, while this would not have occurred in presence of Ca^{2+} for the combination of Ca^{2+} with carboxylic functional groups of BSA [22].

3.2.2. Ionic strength

To investigate the influence of ionic strength on BSA fouling, fouling experiments were performed with NaCl at five different ionic concentrations (1, 10, 30, 60 and 100 mM NaCI). Fig. 3 shows that when the ionic strength increased from 1 to 100 mM NaCl, the water flux reduced from 12.2 to 7.19 LMH, which clearly manifested that BSA fouling became more severe as the ionic strength of the FS increased. It could be attributed to a decrease in the motivation, mainly due to the hydraulic resistance of the fouling layer but in part due to the high osmotic pressure of FS at high ionic strength.

At high ionic strength, the electrostatic repulsion among BSA molecules and between the BSA molecules and the membrane decreased, resulting from the significant reduce in the charges of the membrane surface and BSA molecules due to the double layer compression and charge screening. Consequently, the deposition of BSA molecules onto the membrane surface was greatly enhanced, forming a closely packed BSA fouling layer. The resulting fouling layer provided a significant hydraulic resistance to water flow, and then did weaken the permeate flux severely.

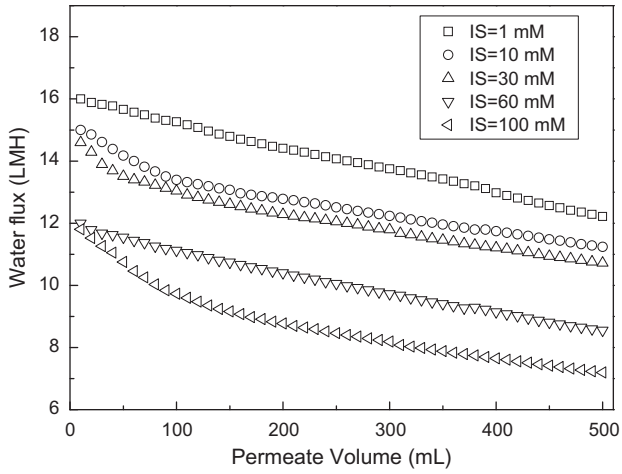

Fig. 3. Effect of ionic strength (IS) on BSA fouling of the FO membrane. Total ionic strength of the FS was adjusted by varying NaCl concentration. No Ca^{2+} was present in the FS.

On the other hand, at low ionic strength, BSA was hard to form thick and compact fouling layer for the strong electrostatic repulsion between the membrane surface and BSA molecules. As a result, of which the decline in product water flux was not as significant as it is at high ionic strength.

3.2.3. Solution pH

The solution pH plays a main role in the charge characteristics of BSA molecules. It will affect the electrostatic interactions among BSA molecules and between BSA molecules and the membrane surface, and then directly influence intermolecular adhesion and foulant deposition on the membrane, which consequently affects membrane fouling. It has been reported that electrostatic interaction is a key factor in controlling protein adsorption behavior on membrane surfaces [23].

The influence of pH on BSA fouling had been investigated at an ionic strength of 10 mM (NaCl), which was in the absence of divalent cation (Ca^{2+}). Results at four different solution pH values (3.44, 4.7, 6.4, and 7.92) are presented in Fig. 4, in which pH 4.7 was the isoelectric point of BSA; pH 6.4 was the ambient (unadjusted) pH; and at pH 3.44 and 7.92, the BSA molecules were positively and negatively charged, respectively. The flux declined most severely at FS pH of 4.7, where the BSA molecules were neutrally charged and had no electrostatic repulsion. The interaction between the neutrally charged BSA molecules was favorable to form a remarkable BSA fouling layer on the membrane. Compared with the flux of

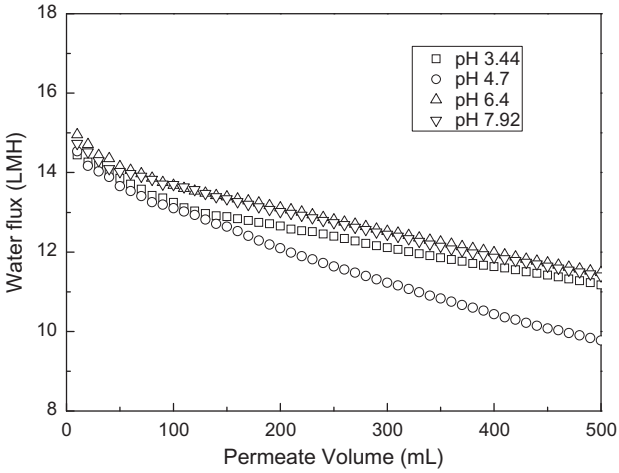

Fig. 4. Effect of solution pH on BSA fouling of the FO membrane. FS pH was adjusted by adding HCl or NaOH stock solutions (0.1 M). No Ca^{2+} was added to the FS.

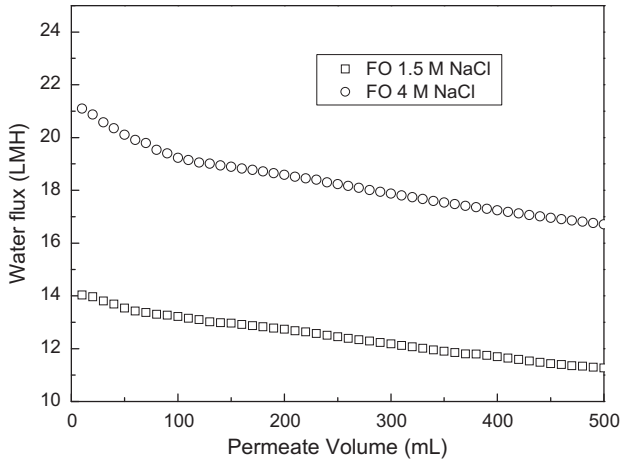

Fig. 5. Effect of initial permeate flux on BSA fouling of the FO membrane. Total ionic strength of the FS was fixed at 10 mM concentration with 0.5 mM Ca^{2+} and 8.5 mM NaCl.

pH 6.4 and 7.92, the flux of pH 3.44 during the initial fouling stage (ca. 150 mL permeate volume after fouling had been initiated) was relatively small. It could be explained by that when the solution pH was 3.44, the electrostatic attraction between the positively charged BSA molecules and the negatively charged membrane surface was conducive to form the fouling layer which resulted in significant flux decline. As time went on, the difference between the flux of pH 3.44, 6.4 and 7.92 tended to narrow. It was attributed to that the electrostatic interactions between BSA molecules and the membrane surface were replaced by those among BSA molecules. There was electrostatic repulsion between the negatively or positively charged BSA molecules.

3.3. Effect of initial permeate flux

The effects of initial flux on the membrane fouling of BSA in the PRO mode had been studied by Mi and Elimelech [15]. They found that the water flux of 4 M NaCl draw declined dramatically during the initial fouling stage (ca. 150 mL permeate volume after fouling had started). Hence, the resulting flux of 4 M NaCl draw was less than that of 1.5 M NaCl. It was attributed mainly to the permeation drag resulting from convective flow toward the membrane. A transition in the fouling layer from a loose fouling layer structure to a much more compact cake layer was the large difference in the fouling behavior with BSA for low and high initial permeate flux. In our work, the effect of initial permeate flux on BSA fouling of FO membrane was conducted in the FO mode. As revealed in Fig. 5, the flux of 4 M NaCl draw was larger than that of 1.5 M NaCl, which was in contrast with the PRO mode. Even though the higher initial flux also caused higher flux decline, the influence is relatively small in the FO mode.

3.4. Effect of membrane orientation

Since there were many differences in performance between the FO and PRO mode, the fouling tests of both FO and PRO mode were conducted. The concentration of DS (NaCl solution) used in FO and PRO mode was 4 and 1.5 M in order to obtain the same

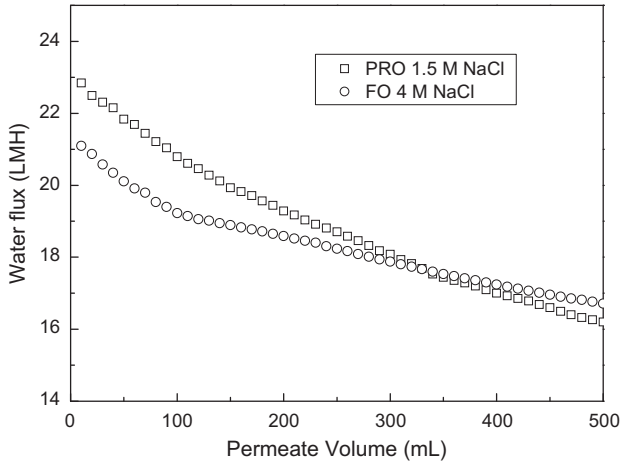

Fig. 6. Effect of membrane orientation on BSA fouling of the FO membrane. The DS contained 4 M NaCl for FO mode and 1.5 M NaCl for PRO mode. Total ionic strength of the FS was fixed at 10 mM concentration with 0.5 mM Ca^{2+} and 8.5 mM NaCl.

initial flux. As shown in Fig. 6, the flux decline is more severe in the PRO mode than in the FO mode. The situation could be explained by the fouling mechanism of BSA. There were two main factors controlling the membrane fouling: chemical and hydrodynamic interactions. Chemical interactions, such as calcium binding, were discussed previously in section 3.2. Hydrodynamic interactions, such as permeation drag and shear force, influenced the deposition and accumulation of foulant molecules on the membrane surface. During membrane fouling, the hydrodynamic conditions presented in the two membrane orientations were different for the asymmetric structure of FO membrane which was characterized by a dense active layer on top of a porous support layer. In the FO mode, with the FS facing the membrane dense active layer, foulant deposited or accumulated on top of the active layer. Which was generally governed by the coupled influence of permeation drag and shear force, resulting from the permeate flux and bulk cross-flow, respectively. However, in the PRO mode, with the FS facing the membrane porous support layer, foulant deposition occurred within the porous structure of the membrane. The influence of hydrodynamic shear forces is vanishing for the absence of cross-flow within the porous support layer. In other words, shear force was precluded as a mechanism to drive foulant away from the membrane. Therefore, cake layer formation due to lack of shear force led to more severe fouling, resulting in marked flux decline with BSA in the PRO mode.

3.5. Influence of feed foulant composition on fouling

Flux behaviors were observed during fouling tests with FSs containing various foulant compositions to investigate the influence of different organic foulant concentrations on fouling. There were three kinds of FS with the total foulant concentration maintained at 200 mg/L, which were (a) 200 mg/L of BSA and no alginate, (b) 140 mg/L BSA and 60 mg/L of alginate, and (c) 60 mg/L BSA and 140 mg/L alginate, respectively. The background electrolyte solution contained 0.5 mM Ca^{2+} and its total ionic strength was fixed at 10 mM by varying NaCl concentration.

As shown in Fig. 7, compared to that in the presence of only BSA foulant, there was a prominent flux decline during fouling in the presence of both BSA and alginate, which indicated that the presence of alginate aggravated the organic fouling. The feed containing only 200 mg/L BSA had the highest flux (10.8 LMH). The alginate molecules were able to form a gel-type fouling layer through the action of intermolecular bridging in the presence of Ca^{2+}. The

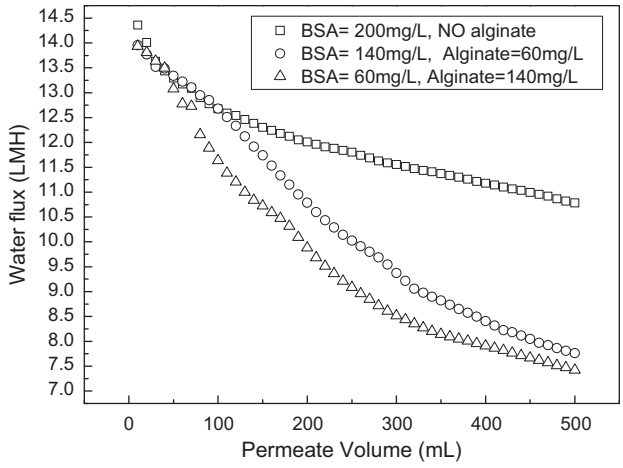

Fig. 7. Effect of feed foulant composition on organic fouling of the FO membrane. Total ionic strength of the FS was fixed at 10 mM concentration with 0.5 mM Ca^{2+} and 8.5 mM NaCl.

gel-like fouling layer would decrease the flux significantly by enhancing the hydraulic resistance. Although BSA molecules could also interact with Ca^{2+} and forming complexes, compared to the alginate, the content of carboxylic groups in BSA molecules was low, which greatly reduced the possibility of forming a cross-linked layer.

Moreover, as expected, the flux-decline profiles varied correspondingly to the proportions of BSA to alginate. Specifically, the decline of flux was more severe with the increase in the concentration of alginate for the significant extent of gel formation at high alginate concentration. Interestingly, the difference of flux between the two kinds of co-foulants (BSA and alginate) was declining. There was a possible explanation for this behavior. In the presence of alginate, the BSA molecules playing as co-foulant enhanced the fouling by cross-linking with the alginate–calcium complex, resulting in a fouling layer which had similar hydraulic resistance to that of a fouling layer of alginate–calcium complexes.

3.6. Characteristics of CTA FO membrane

To further investigate the fouling of the membrane, membrane coupons after FO run were taken out from the membrane cell and observed using SEM. The membranes of the fouling tests (200 mg/L BSA) under the different conditions of (a) 2 mM Ca^{2+} and 4 mM NaCl, (b) 0.5 mM Ca^{2+} and 8 mM NaCl, (c) pH 4.7 and 10 mM NaCl, (d) combined fouling of 60 mg/L BSA and 140 mg/L alginate (instead of 200 mg/L BSA) and 0.5 mM Ca^{2+} and 8 mM NaCl, (e) IS = 1 mM

and (f) IS = 100 Mm were chosen as representative. The active layer SEM images of fouling membrane are shown in Fig. 8. It can be clearly seen that the six membranes suffered contamination in different extent. Fig. 8(a) and (b) elucidated clearly that the increase of the Ca^{2+} concentration promoted the formation of complexes, and then led to more severe membrane fouling, which was in accordance with the results in section 3.2.1. The membrane fouling in pH 4.7 was relatively serious for the neutrally charged BSA molecules where there was no electrostatic repulsion among themselves (Fig. 8(c)). The combined fouling of BSA and alginate was grave, where most of the foulant was in the form of folding sheets, which was shown in Fig. 8(d). It was mainly attributed to the action of intermolecular bridging between the carboxylic groups in alginate molecules and the divalent ion Ca^{2+}, forming a cross-linked foulant layer, which had been described in detail in section 3.5. The adsorption caused blocking of the surface membrane pores and led to severe flux reduction. Comparing Fig. 8(e) and (f), we found that high ionic strength was in favor of the formation of foulant and it confirmed the condition in section 3.6.

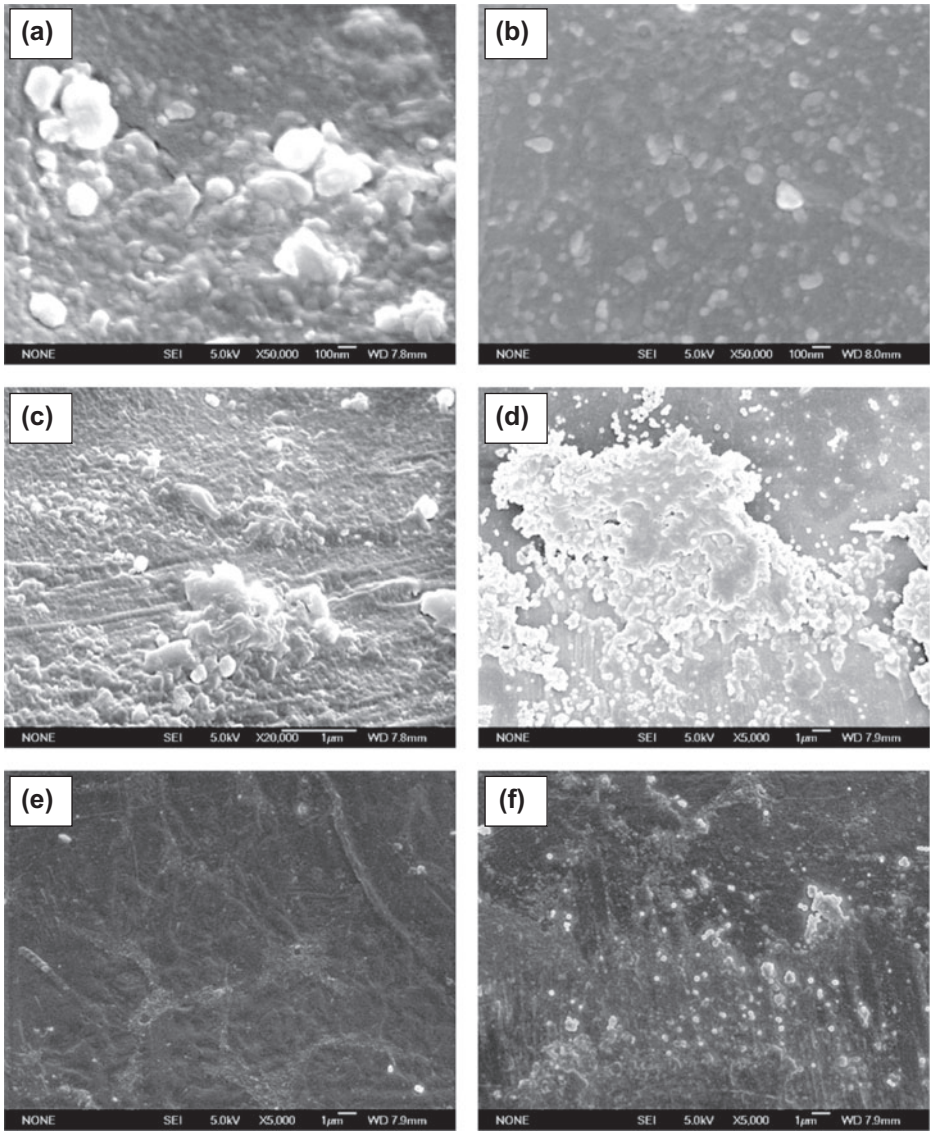

Fig. 8. SEM images of membrane fouled under the different conditions of the (a) 2 mM Ca^{2+} and 4 mM NaCl, (b) 0.5 mM Ca^{2+} and 8 mM NaCl, (c) pH 4.7 and 10 mM NaCl, (d) combined fouling of 60 mg/L BSA and 140 mg/L alginate and 0.5 mM Ca^{2+} and 8 mM NaCl, (e) IS = 1 mM and (f) IS = 100 Mm.

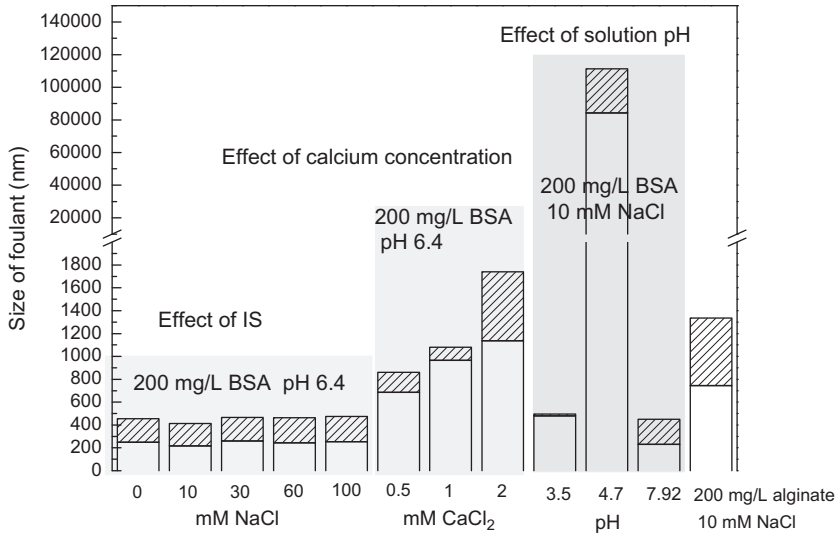

Fig. 9. The size distribution of foulant molecules in various kinds of FS.

Moreover, some of foulants were in the form of spherality, which was the inorganic fouling for the NaCl molecules. It had been proven by V. Parida and Ng that the organic foulants commonly possessed irregular and random structures, while the inorganic foulant salts had a well-defined crystalline structure [24].

3.7. Size distribution of foulant molecules

Since calcium enhanced FO fouling by interacting and forming complexes with carboxylic functional groups of organic molecules, the size distribution of foulant molecules in various FS was measured. As presented in Fig. 9, there was no significant difference among the foulant size under different ionic strengths, which indicated that the IS had less impact on electrostatic interactions among BSA molecules. The decline of flux in the high IS was mainly attributed to the enhanced deposition of BSA molecules onto the membrane surface. Furthermore, BSA size increased with the increasing of Ca^{2+} concentration, which was consistent with the analysis in section 3.2.1. The size of BSA at pH 4.7 was extremely large since that

BSA molecule has no electrostatic charge and minimum solubility at isoelectric point. The size of foulant at FSs can be used as a reference to judge and control the behavior of organic fouling. However, it cannot be the only criteria.

4. Conclusion

This study was concentrated on membrane fouling mechanisms of protein during the FO process. BSA was chosen as a representative protein of secondary wastewater effluent. The effect of physical and chemical interactions, such as calcium concentration, ionic strength, pH, feed foulant composition, initial permeate flux and membrane orientation on membrane fouling was discussed in the FO process.

The result of fouling tests indicated that Ca^{2+} promoted the formation of BSA–Ca^{2+} complexes and then enhanced the membrane fouling. Higher deposition of BSA was also observed when the ionic strength of FS increased due to the decreased electrostatic repulsion. Solution pH played a vital part on the membrane fouling of BSA through electrostatic interaction. Fouling became much more significant at pH 4.7 (the BSA isoelectric point). It was also demonstrated that the presence of alginate (a model polysaccharide) as co-foulant aggravated the BSA fouling of FO membrane for the formation of alginate–BSA–Ca^{2+} complexes within the fouling layer increased the total membrane resistance. Furthermore, membrane orientation played an important role on membrane fouling, where the fouling in the PRO mode was more severe than that in the FO mode. In addition, the SEM image of fouled membrane and the size distribution of foulant molecules was measured and used as a support to judge the fouling behavior.

References

[1] M.A. Shannon, P.W. Bohn, M. Elimelech, J.G. Georgiadis, B.J. Marinas, A.M. Mayes, Science and technology for water purification in the coming decades, Nature 452 (2008) 301–310.

[2] L.A. Hoover, W.A. Phillip, A. Tiraferri, N.Y. Yip, M. Elimelech, Forward with osmosis: Emerging applications for greater sustainability, Environ. Sci. Technol. 45 (2011) 9824–9830.

[3] T.-S. Chung, X. Li, R.C. Ong, Q. Ge, H. Wang, G. Han, Emerging forward osmosis (FO) technologies and challenges ahead for clean water and clean energy applications, Curr. Opin. Chem. Eng. 1 (2012) 246–257.

[4] S. Zhang, P. Wang, X. Fu, T.S. Chung, Sustainable water recovery from oily wastewater via forward osmosis-membrane distillation (FO-MD), Water Res. 52 (2014) 112–121.

[5] C. Boo, M. Elimelech, S. Hong, Fouling control in a forward osmosis process integrating seawater desalination and wastewater reclamation, J. Membr. Sci. 444 (2013) 148–156.

[6] Y. Wang, F. Wicaksana, C.Y. Tang, A.G. Fane, Direct microscopic observation of forward osmosis membrane fouling, Environ. Sci. Technol. 44 (2010) 7102–7109.

[7] K. Jim, A. Fane, C. Fell, D. Joy, Fouling mechanisms of membranes during protein ultrafiltration, J. Membr. Sci. 68 (1992) 79–91.

[8] J.L. Nilsson, Protein fouling of UF membranes: Causes and consequences, J. Membr. Sci. 52 (1990) 121–142.

[9] A. Marshall, P. Munro, G. Trägårdh, The effect of protein fouling in microfiltration and ultrafiltration on permeate flux, protein retention and selectivity: A literature review, Desalination 91 (1993) 65–108.

[10] C.-C. Ho, A.L. Zydney, Effect of membrane morphology on the initial rate of protein fouling during microfiltration, J. Membr. Sci. 155 (1999) 261–275.

[11] W. Bowen, J. Calvo, A. Hernandez, Steps of membrane blocking in flux decline during protein microfiltration, J. Membr. Sci. 101 (1995) 153–165.

[12] W. Ang, M. Elimelech, Protein (BSA) fouling of reverse osmosis membranes: Implications for wastewater reclamation, J. Membr. Sci. 296 (2007) 83–92.

[13] S. Lee, C. Boo, M. Elimelech, S. Hong, Comparison of fouling behavior in forward osmosis (FO) and reverse osmosis (RO), J. Membr. Sci. 365 (2010) 34–39.

[14] B. Mi, M. Elimelech, Chemical and physical aspects of organic fouling of forward osmosis membranes, J. Membr. Sci. 320 (2008) 292–302.

[15] B. Mi, M. Elimelech, Organic fouling of forward osmosis membranes: Fouling reversibility and cleaning without chemical reagents, J. Membr. Sci. 348 (2010) 337–345.

[16] J. Peula-Garcia, R. Hidaldo-Alvarez, F. De las Nieves, Protein co-adsorption on different polystyrene latexes: Electrokinetic characterization and colloidal stability, Colloid Polym. Sci. 275 (1997) 198–202.

[17] X. Jin, Q. She, X. Ang, C.Y. Tang, Removal of boron and arsenic by forward osmosis membrane: Influence of membrane orientation and organic fouling, J. Membr. Sci. 389 (2012) 182–187.

[18] C.Y. Tang, Q. She, W.C.L. Lay, R. Wang, A.G. Fane, Coupled effects of internal concentration polarization and fouling on flux behavior of forward osmosis membranes during humic acid filtration, J. Membr. Sci. 354 (2010) 123–133.

[19] P. Zhao, Q. Yue, B. Gao, J. Kong, H. Rong, P. Liu, H.K. Shon, Q. Li, Influence of different ion types and membrane orientations on the forward osmosis performance, Desalination 344 (2014) 123–128.

[20] J.R. McCutcheon, M. Elimelech, Influence of concentrative and dilutive internal concentration polarization on flux behavior in forward osmosis, J. Membr. Sci. 284 (2006) 237–247.

[21] G.I. Loeb, H.A. Scheraga, Hydrodynamic and thermodynamic properties of bovine serum albumin at low pH, J. Phys Chem. 60 (1956) 1633–1644.

[22] S.T. Kelly, A.L. Zydney, Mechanisms for BSA fouling during microfiltration, J. Membr. Sci. 107 (1995) 115–127.

[23] J. Brinck, A.S. Jönsson, B. Jönsson, J. Lindau, Influence of pH on the adsorptive fouling of ultrafiltration membranes by fatty acid, J. Membr. Sci. 164 (2000) 187–194.

[24] V. Parida, H.Y. Ng, Forward osmosis organic fouling: Effects of organic loading, calcium and membrane orientation, Desalination 312 (2013) 88–98.